


Cite this: *Nanoscale Adv.*, 2019, 1, 299

# On the solution structure of kraft lignin in ethylene glycol and its implication for nanoparticle preparation

Mingkun Yang,<sup>a</sup> Wenwen Zhao,<sup>a</sup> Seema Singh,<sup>b</sup> Blake Simmons<sup>cd</sup> and Gang Cheng<sup>id \*a</sup>

Received 15th June 2018  
Accepted 25th August 2018

DOI: 10.1039/c8na00042e

rsc.li/nanoscale-advances

## Introduction

As the main renewable source of aromatic compounds, lignin has lately attracted researchers' interest to develop high-value added products such as lignin-derived platform chemicals and lignin-based nonmaterial for biomedical applications, *etc.*<sup>1–4</sup> Lignin is synthesized *in planta* by cross-coupling reactions of phenolic radicals produced from three monomers: coniferyl alcohol (G unit), sinapyl alcohol (S unit) and *p*-coumaryl alcohol (H unit). Lignin possesses complex structures which can only be described by structural motifs and chemical linkages.<sup>5,6</sup> Its inherent structural heterogeneity is further compounded by different extraction processes that often modify the native structure.<sup>2</sup> Extracted lignins often contain structurally different fractions. Several recent studies fractionated softwood kraft lignin using acetone and reported different properties of acetone soluble lignin (ASL) and acetone insoluble lignin (AIL).<sup>7–9</sup> The initial lignin sample was found to contain about 65–70 wt% of ASL, and the AIL was about 35–30 wt%. It was suggested that higher molecular weight AIL contains extensive  $\pi$ -stacking.<sup>8</sup> The phenolic-OH content in ASL is higher than that in AIL, and this correlates with its better anti-oxidant properties.<sup>7</sup> High value application of lignin is hampered by its

structural complexity and variability, which also present a challenge for characterization.<sup>10–12</sup> Computer simulation<sup>13–16</sup> and neutron scattering<sup>16–22</sup> have been recently applied to understand the structure and dynamics of lignin in solutions and in the solid state. Knowledge derived from these studies helps to understand the behaviors of lignin during biomass pretreatments<sup>13,14,17,22</sup> and guide rationally improving lignin processing.<sup>15,19</sup>

Lignin nanoparticles are rapidly being realized as a means to bestow value upon lignin.<sup>23–28</sup> They are usually fabricated by dissolution of lignin that is followed by changes in solvent quality.<sup>23</sup> The process of nanoparticle synthesis can be described in terms of nucleation and growth. The growth of nanoparticles in solutions occurs by several mechanisms including: diffusion controlled growth and coalescence, *etc.*<sup>29</sup> In a mechanistic study of lignin nanoparticle preparation, the mechanism of nanoparticle growth was compared with diffusion controlled growth.<sup>30</sup> Synthesis of lignin nanoparticles with well-defined sizes *via* a scalable process is essential to promote its widespread application.<sup>31</sup> Concentrated lignin solutions are also necessary for scaling up nanoparticle production,<sup>31</sup> which calls for robust lignin solvents with a high solubility. This requires a clear understanding of the nature of interactions between solvent molecules and lignin, the resultant solution structure and the factors that control nanoparticle formation.<sup>23,30,32</sup>

Recently, ethylene glycol (EG) is drawing attention as a lignin solvent that can dissolve as much as 70 wt% alkali lignin.<sup>33</sup> EG has been used to prepare nanoparticles from its lignin solutions and these nanoparticles exhibit interesting antioxidant, anti-microbial and anti-corrosive properties.<sup>24,27,28,30</sup> However, the solution structure of lignin in EG has not been reported<sup>30</sup> and nanoparticles with a well-defined size and shape are not always

<sup>a</sup>State Key Laboratory of Organic-Inorganic Composites, College of Life Science and Technology, Beijing University of Chemical Technology, North 3rd Ring East, # 15, Beijing, 100029, China. E-mail: gchengbuct@gmail.com; chenggang@mail.buct.edu.cn

<sup>b</sup>Biomass Science and Conversion Technology Department, Sandia National Laboratories, 7011 East Avenue, Livermore, CA 94551, USA

<sup>c</sup>Joint BioEnergy Institute (JBEI), 5885 Hollis Street, Emeryville, CA 94608, USA

<sup>d</sup>Biological Systems and Engineering Division, Lawrence Berkeley National Laboratory, Berkeley, 94702, CA, USA



obtained from EG solutions.<sup>25</sup> In a previous study, Indulin AT lignin was dissolved in EG and nanoparticles were formed after an induced pH drop.<sup>30</sup> The solution structure of lignin in EG prior to the pH drop was not investigated in that work. In another study, Sigma-Aldrich kraft lignin was dissolved in EG and EG was then replaced with water *via* dialysis.<sup>25</sup> However, no nanoparticles with a well-defined shape and size were observed in aqueous media. This work tried to establish a connection between the lignin solution structure and lignin nanoparticle preparation. In this work, small angle neutron scattering (SANS) and dynamic light scattering (DLS) are used to better understand the interactions between EG and kraft lignin, the solution structures of lignin in EG and the process of lignin nanoparticle preparation.

## Experimental section

### Materials

Kraft lignin (product number 370959, batch number MKBS2568V) was purchased from Sigma-Aldrich. EG and DMSO were also purchased from Sigma-Aldrich. Deuterated DMSO was purchased from Cambridge Isotope Laboratories, Inc. Deuterated EG was purchased from Alfa Aesar.

### SANS

The SANS measurements were performed at the National Institute of Standards and Technology (NIST). The experiment at the NIST was carried out on the NGB 30 m beamline of the Cold Neutron Research Facility. Three SDDs (1.33, 4.0 and 13.17 m) with a detector offset of 25 cm at 1.33 m and a neutron

wavelength of  $\lambda = 6 \text{ \AA}$  were used to cover scattering vectors ranging from 0.004 to  $0.45 \text{ \AA}^{-1}$ . The scattering intensity was put on an absolute scale by calibration with a direct beam flux. Samples for measurement at  $25^\circ\text{C}$  were loaded into quartz cells with a thickness of 2.0 mm. The NCNR software package for SANS data analysis ([https://www.ncnr.nist.gov/programs/sans/data/red\\_anal.html](https://www.ncnr.nist.gov/programs/sans/data/red_anal.html)) was used in this study.

### DLS

The particle size of the lignin nanoparticles was measured with a Malvern Zetasizer Nano-ZS90 Instrument. Measurements were repeated three times for each sample to check the reproducibility.

## Results and discussion

Lignin may exist in two states in solutions: individual lignin subunits and their aggregates.<sup>23</sup> The kraft lignin studied here has an  $M_n$  of 2300 and an  $M_w$  of  $4600 \text{ g mol}^{-1}$  measured from acetylated lignin in THF using size exclusion chromatography (Waters 1525, Milford, MA, USA) and polystyrene as a standard. The composition and chemical structure of a similar lignin (same batch number, different bottles) were studied by a number of techniques including HSQC-NMR and 2D NMR and the results were presented in our previous paper.<sup>21</sup> Fig. 1a presents SANS data from EG solutions of lignin with different concentrations: 0.6, 2.3, 4.6, 8.8 and 13.0 wt%. The solutions were kept at room temperature for one week prior to SANS measurement. SANS data exhibit an upturn in the low- $q$  region which indicates the presence of larger aggregates. In a SANS

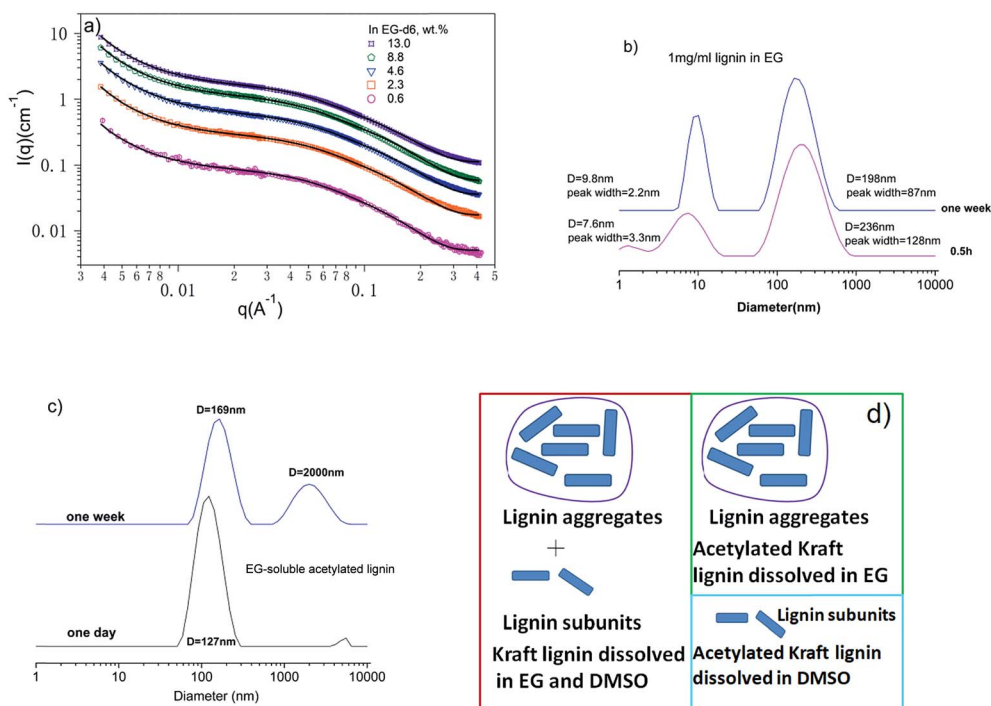


Fig. 1 (a) SANS data of lignin in EG with different concentrations. The solid lines are a fit to eqn (1). (b) DLS data of  $1 \text{ mg ml}^{-1}$  lignin in EG. (c) DLS data of dissolved acetylated lignin in EG. (d) Schematic illustrations of the solution structures of lignin and acetylated lignin in EG and DMSO.



experiment, the size of a structure, for example, the radius of gyration of an object, is resolved reliably if  $R_g \times q_{\min} \leq 1$ . The  $q_{\min}$  represents the lowest  $q$  value reached in the experiment.<sup>34</sup> Here, the aggregates are too large (>100 nm) to be fully resolved by SANS conducted in this work and the low- $q$  upturn corresponds to only a portion of the whole structure.<sup>35</sup>

The scattering due to lignin subunits dominates the intermediate to high  $q$  region. DLS data of 0.1 wt% EG solution (Fig. 1b) confirms the co-existence of small and large particles. It is observed that lignin's solution structure is dynamic, a phenomenon that has been reported before.<sup>36,37</sup> The solution structure becomes stable after one week, and the DLS data show that small particles have a hydrodynamic diameter of 9.5 nm and large ones have an average diameter of 198 nm. The small particles correspond to lignin subunits with a measured  $M_w$  of  $4600 \text{ g mol}^{-1}$ .<sup>23</sup>

The main interacting forces that hold lignin subunits together have been identified as hydrogen bonding between hydroxyl groups<sup>38</sup> and  $\pi$ - $\pi$  interactions<sup>39</sup> between phenyl rings. To dissolve lignin, the interactions between solvent molecules and lignin subunits need be strong enough to overcome the inter-molecular hydrogen bonding and  $\pi$ - $\pi$  interactions. Hydrogen bonding has been proposed as the molecular interaction between EG and lignin.<sup>33,40</sup> This is supported by the low solubility of acetylated lignin in EG. Studies have shown that lignin phenolic and aliphatic hydroxyl groups are acetylated during lignin acetylation,<sup>41</sup> and therefore its ability to form hydrogen bonds with EG should be greatly reduced. It is observed that only a fraction of 40 mg of acetylated lignin is soluble in 10 ml of EG after mixing them for one day. DLS data of the soluble portion show only large aggregates with diameters around 127 nm and they aggregate further with increasing time (Fig. 1c). The remaining solubility is likely due to incomplete acetylation of lignin and the residual hydroxyl groups can form hydrogen bonds with EG.

To have a deeper understanding of different molecular interactions involved in lignin dissolution, acetylated lignin is also mixed with DMSO. In contrast, acetylated lignin is readily soluble in DMSO. SANS of acetylated lignin in DMSO shows no large aggregates.<sup>21</sup> This implies that hydrogen bonding is not the main mechanism by which lignin and acetylated lignin dissolve in DMSO. DMSO interacts with phenyl rings *via* dipole/quadrupole moment interactions,<sup>42</sup> thereby breaking  $\pi$ - $\pi$  interactions between phenyl rings in lignin. However, there are still aggregates in DMSO solutions as shown in our previous work.<sup>21</sup> The absence of aggregates from acetylated lignin in DMSO is attributed to two additional aspects: (1) acetylated lignin contains a number of carbonyl groups which interact with DMSO *via* dipole/dipole interactions,<sup>38</sup> which will increase the interaction between DMSO and acetylated lignin; (2) acetylation of lignin removes most of the inter-molecular hydrogen bonds in lignin, which will decrease the interaction between lignin subunits. Based on the above analysis, it is concluded that hydrogen bonding is not a necessary force for lignin to become soluble in DMSO. Schematic illustrations of the solution structures of lignin and acetylated lignin in EG and DMSO are presented in Fig. 1d.

The conformation of lignin subunits in solutions depends on solvent quality, the degree of branching and molecular weight. A range of structures are possible for lignin subunits including random coil, compact particles, and soft microgel particles.<sup>18,43,44</sup> In a previous simulation study, 61 G units were polymerized without imparting branching and a globular to flexible coil transition was observed with increasing solvent quality.<sup>13</sup> It is not surprising to observe such a transition for a linear polymer chain although it is relatively rigid due to the presence of phenyl rings on the main chain. Flexible linear polymers adopt an expanded coil conformation in a good solvent while they collapse into compact globules in a bad solvent.<sup>45</sup> Experimentally, this transition has not been reported for lignin by SANS in part due to the influence of aggregates of lignin subunits. A globular conformation corresponds to collapsed polymer coils in a poor solvent which can also be described as ellipsoids.<sup>14</sup> Lignin subunits in DMSO have been characterized as rigid cylinders or ellipsoids in previous SANS studies.<sup>17,19–21</sup> This does not necessarily mean that the lignin subunits are collapsed in DMSO since the degree of branching is not known. Branched polymers can assume a cylindrical shape in good solvents.<sup>46</sup> Measuring the degree of branching of lignin subunits is not trivial and it requires extensive NMR studies.<sup>8,47</sup> A recent NMR study of milled wood lignin isolated from spruce (*Picea abies* and *Picea mariana*) and beech (*Fagus*) wood concluded that these lignin samples are linear oligomers rather than network polymers.<sup>47</sup> In a subsequent study, soft-wood kraft lignin is found to consist of two fractions; the ASL is described as a more branched and less polymeric material and the AIL is characterized as a less branched polymeric material. Both of them contain new chemical structures introduced during the extraction process.<sup>8</sup>

The SANS data are quantitatively analyzed using an empirical equation (eqn (1)) that considers contributions from both aggregates and subunits:<sup>21</sup>

$$I(q) = \frac{A}{q^n} + BP(q) + bkg \quad (1)$$

where  $A/q^n$  is due to scattering from aggregates;  $P(q)$  represents the form factor of a lignin subunit.<sup>21</sup>  $A$  and  $B$  are coefficients. The polydispersity of the radius ( $\sigma$ ) of the cylinders was fixed at 0.25. Although a unique value of the exponent  $n$  cannot be obtained due to the limited  $q$  range measured, a value of 2.2 was found to best fit the data. The exponent may not be physically meaningful due to the limited  $q$  range. It is noted that it has been explained as a reflection of compactness of the aggregates in other studies.<sup>20</sup> The subunits are modeled as rigid cylinders here and the results are shown in Table 1. The form factor of a rigid cylinder with a cross-section radius  $R$  and length  $L$  is given as follows:<sup>48</sup>

$$P(q) = \int_0^{\pi/2} |F(q, \cos \theta)|^2 \sin \theta d\theta \quad (2)$$

where  $F(q, \theta) = 2(\rho_{\text{cyl}} - \rho_{\text{soln}})V_{\text{cyl}}j_0(qH \cos \theta) \left[ \frac{J_1(qR \sin \theta)}{qR \sin \theta} \right]$ ,  $H = L/2$ ,  $j_0(x) = \sin x/x$ , and  $J_1$  is the first-order cylindrical Bessel



Table 1 Results of SANS data analysis

Lignin concentration in EG (wt%)	Cross-sectional radius $R$ (Å)	Cylinder length $L$ (Å)	Cylinder volume (Å <sup>3</sup> )	Reduced $\chi^2$
0.6	8	83	$17.7 \times 10^3$	1.5
2.3	8	82	$17.5 \times 10^3$	3.1
4.2	8	83	$17.7 \times 10^3$	4.9
8.8	8	86	$18.3 \times 10^3$	7.2
13.0	8	87	$18.5 \times 10^3$	7.4

function,  $V_{\text{cyl}} = \pi R^2 L$ , and  $\theta$  is the angle between the cylinder axis and the scattering vector  $q$ .

Assuming a Schulz distribution of cross-sectional radius  $R$ :

$$f(R) = \frac{R^z}{\Gamma(z+1)} \left( \frac{z+1}{\langle R \rangle} \right)^{z+1} \exp \left[ -\frac{R(z+1)}{\langle R \rangle} \right] \quad (3)$$

The polydispersity  $\sigma$  is given as  $\sigma^2 = 1/(z+1)$ .

The averaged form factor is then given as

$$\overline{P(q)} = \int P(q)f(R)dr \quad (4)$$

The length of cylinders is  $\sim 80$  Å and this corresponds to about 10 monolignol units assuming that the length of one phenyl propane unit is  $\sim 8$  Å. This is roughly consistent with an  $M_n$  of  $2300 \text{ g mol}^{-1}$  considering the average monomer molecular weight (the C9 unit),  $190\text{--}200 \text{ g mol}^{-1}$ .<sup>47,49</sup> Cylinders with similar length scales have been reported in previous SANS studies of lignin subunits.<sup>19–21</sup> The cross-sectional radius of the cylinders is  $\sim 8$  Å. Therefore these cylinders are considered as short cylinders and the overall shape of the lignin subunits is elongated.<sup>17</sup>

It is noted that the value of reduced  $\chi^2$ , an indication of the quality of the fitting, increases with increasing solution concentration from 1.5 to 7.4. A lower value indicates a better fit. A closer look at the data shows that the model deviates from the data in the higher  $q$  region from 0.3 to 0.4 Å<sup>−1</sup>. This implies

that the lignin subunits are not compact particles. In addition, the SANS data do not level off in the high  $q$  region which indicates the presence of smaller structures. Considering small sizes of lignin subunits, more accurate determination of the conformation of lignin subunits requires extension of the high  $q$  limit to around  $1 \text{ Å}^{-1}$ .<sup>50,51</sup> In addition, the knowledge of the degree of branching of lignin subunits will also provide complimentary information to interpret the SANS data.

The size of lignin subunits is weakly dependent on lignin concentration. This suggests that the solvent quality of EG is in the poor solvent region but close to the theta solvent and the interactions between lignin subunits in EG are small.<sup>46</sup> Therefore, EG is not considered as a good solvent although it can dissolve a significant amount of lignin. The aggregation in dilute solutions of EG indicates that EG is also not a real theta solvent for lignin and the EG-mediated interactions between lignin subunits are small but attractive.

EG is particular attractive as a lignin solvent for the preparation of nanoparticles due to its high kraft lignin solubility. As mentioned earlier, nanoparticles with a well-defined shape and size were not produced from EG solutions in one study.<sup>25</sup> This is in contrast with other studies where lignin nanoparticles were obtained from EG solutions of Sigma-Aldrich kraft lignin,<sup>28</sup> Indulin AT lignin<sup>30</sup> and steam-exploded rice straw lignin.<sup>27</sup> Lignin nanoparticles with well-defined sizes were obtained from EG solutions by introducing 0.01 M HCl solution, as shown in Fig. 2a. After addition of 1.5 ml of 0.01 M HCl solution to 5 ml of  $1 \text{ mg ml}^{-1}$  lignin solution and being kept at room temperature for one week, the solution contains only one population of particles with diameters around 152 nm and a much smaller peak width, 30 nm. Nanoparticles are stabilized by surface charges in solutions.<sup>25,30</sup> In this work, they are stable in  $1 \text{ mg ml}^{-1}$  EG solutions for more than one week because of a lower chance of collision with each other. The lignin nanoparticles can be transferred to aqueous solutions *via* dialysis where they are stable up to a few months because of ionization of phenolic hydroxyl and carbonyl groups.<sup>25,30,32</sup>

The process of nanoparticle formation is affected by many factors such as lignin and the solvent type, the initial lignin concentration, the amount and rate of anti-solvent addition,

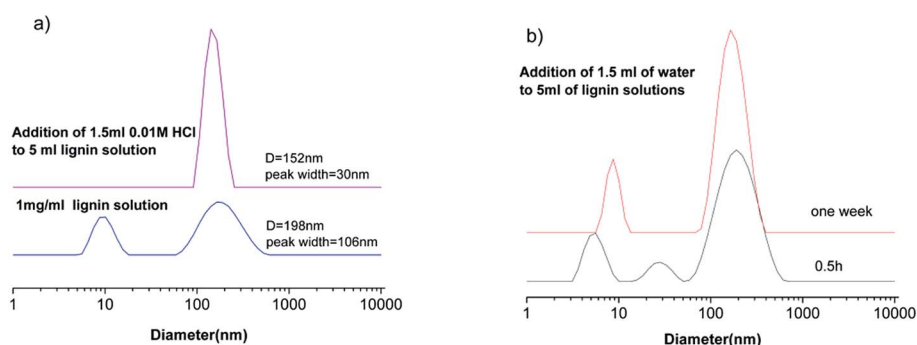


Fig. 2 (a) DLS data of the  $1 \text{ mg ml}^{-1}$  lignin solution and the lignin solution after addition of 1.5 ml of HCl. Both of the samples were kept at room temperature for one week before DLS measurement. (b) Addition of 1.5 ml of water to 5 ml of  $1 \text{ mg ml}^{-1}$  lignin solutions which were kept at room temperature for 0.5 h and one week, respectively. Both of the samples were kept at room temperature for 6 h after addition of anti-solvents before DLS measurement.





temperature, *etc.*<sup>26,30–32</sup> DLS data here show that both the lignin subunits and pre-existing aggregates are involved in the process of nanoparticle formation. Whether the pre-existing aggregates affect the size of the obtained nanoparticles will depend on the relative amount of subunits and aggregates. SANS data suggest that pre-existing aggregates are the minor component in the EG solution due to small attractive interactions. Therefore their influence on nanoparticle preparation seems to be small. If the pre-existing aggregates dominate the lignin solution, the obtained nanoparticles will certainly be affected by them. In addition, the process of nanoparticle formation is also affected by the dynamic nature of lignin solutions. Fig. 2b shows that different solution structures are obtained upon addition of water to the EG solutions which were kept at room temperature for half an hour and one week after preparation. This will also add variability to the obtained lignin nanoparticles. Therefore, one needs take into account the dynamic nature of lignin solutions.

## Conclusions

In this work, we further discussed the mechanism of lignin solubilization in EG and DMSO based on previous findings and our current results. A comparison between the solubility of acetylated lignin in EG and DMSO further supported the notion that hydrogen bond formation between lignin and EG is the main driving force for its dissolution. The results also concluded that hydrogen bonding is not a necessary force for lignin to become soluble in DMSO, a conclusion that could not be reached in our previous paper. The solvent quality of EG for kraft lignin is close to the theta solvent from the poor solvent side. The overall shape of lignin subunits is described as rigid cylinders according to SANS data; however lignin subunits are not compact particles. Aggregation of lignin subunits in EG occurs due to slightly attractive interactions between lignin subunits.

Lignin nanoparticles are obtained by adding anti-solvents to EG solutions and the dynamic solution structure affects the obtained nanoparticles. The results present a clearer picture of the solution structure of lignin in EG and will help to understand the process of lignin nanoparticle preparation.

## Conflicts of interest

The authors declare no competing financial interest.

## Acknowledgements

We thank Dr Boualem Hammouda (NCNR, NIST) for his discretionary neutron beam time and Mr Cedric Gannon (NCNR, NIST) for the help with the SANS experiment. Gang Cheng acknowledges support for this research by the National Natural Science Foundation of China (U1432109) and China Scholarship Council (201606885004). The work carried out at the DOE Joint BioEnergy Institute (<http://www.jbei.org>) was supported by the U. S. Department of Energy, Office of Science, Office of Biological and Environmental Research, through

contract DE-AC02-05CH11231 between the Lawrence Berkeley National Laboratory and the U. S. Department of Energy. Access to NGB 30 m SANS was provided by the Center for High Resolution Neutron Scattering, a partnership between the National Institute of Standards and Technology and the National Science Foundation under Agreement No. DMR-1508249. We acknowledge the support of the National Institute of Standards and Technology, U.S. Department of Commerce, in providing the neutron research facilities used in this work.

## References

- 1 Z. Sun, B. Fridrich, A. de Santi, S. Elangovan and K. Barta, *Chem. Rev.*, 2018, **118**, 614–678.
- 2 W. Schutyser, T. Renders, S. Van den Bosch, S. F. Koelewijn, G. T. Beckham and B. F. Sels, *Chem. Soc. Rev.*, 2018, **47**, 852–908.
- 3 P. Figueiredo, K. Lintinen, J. T. Hirvonen, M. A. Kostainen and H. A. Santos, *Prog. Mater. Sci.*, 2018, **93**, 233–269.
- 4 D. Kun and B. Pukánszky, *Eur. Polym. J.*, 2017, **93**, 618–641.
- 5 R. Rinaldi, R. Jastrzebski, M. T. Clough, J. Ralph, M. Kennema, P. C. A. Bruijninx and B. M. Weckhuysen, *Angew. Chem., Int. Ed.*, 2016, **55**, 8164–8215.
- 6 S. Constant, H. L. J. Wienk, A. E. Frissen, P. d. Peinder, R. Boelens, D. S. van Es, R. J. H. Grisel, B. M. Weckhuysen, W. J. J. Huijgen, R. J. A. Gosselink and P. C. A. Bruijninx, *Green Chem.*, 2016, **18**, 2651–2665.
- 7 H. Sadeghifar and D. S. Argyropoulos, *ACS Sustainable Chem. Eng.*, 2015, **3**, 349–356.
- 8 C. Crestini, H. Lange, M. Sette and D. S. Argyropoulos, *Green Chem.*, 2017, **19**, 4104–4121.
- 9 H. Sadeghifar and D. S. Argyropoulos, *ACS Sustainable Chem. Eng.*, 2016, **4**, 5160–5166.
- 10 J. S. Lupoi, S. Singh, R. Parthasarathi, B. A. Simmons and R. J. Henry, *Renewable Sustainable Energy Rev.*, 2015, **49**, 871–906.
- 11 J. L. Wen, S. L. Sun, B. L. Xue and R. C. Sun, *Materials*, 2013, **6**, 359–391.
- 12 H. Lange, F. Rulli and C. Crestini, *ACS Sustainable Chem. Eng.*, 2016, **4**, 5167–5180.
- 13 M. D. Smith, B. Mostofian, X. Cheng, L. Petridis, C. M. Cai, C. E. Wyman and J. C. Smith, *Green Chem.*, 2016, **18**, 1268–1277.
- 14 L. Petridis, R. Schulz and J. C. Smith, *J. Am. Chem. Soc.*, 2011, **133**, 20277–20287.
- 15 D. Vural, C. Gainaru, H. O'Neill, Y. Pu, M. D. Smith, J. M. Parks, S. V. Pingali, E. Mamontov, B. H. Davison, A. P. Sokolov, A. J. Ragauskas, J. C. Smith and L. Petridis, *Green Chem.*, 2018, **20**, 1602–1611.
- 16 A. J. Ragauskas, G. T. Beckham, M. J. Biddy, R. Chandra, F. Chen, M. F. Davis, B. H. Davison, R. A. Dixon, P. Gilna, M. Keller, P. Langan, A. K. Naskar, J. N. Saddler, T. J. Tschaplinski, G. A. Tuskan and C. E. Wyman, *Science*, 2014, **344**, 1246843.
- 17 G. Cheng, M. S. Kent, L. He, P. Varanasi, D. Dibble, R. Arora, K. Deng, K. Hong, Y. B. Melnichenko, B. A. Simmons and S. Singh, *Langmuir*, 2012, **28**, 11850–11857.



- 18 S. E. Harton, S. V. Pingali, G. A. Nunnery, D. A. Baker, S. H. Walker, D. C. Muddiman, T. Koga, T. G. Rials, V. S. Urban and P. Langan, *ACS Macro Lett.*, 2012, **1**, 568–573.
- 19 A. E. Imel, A. K. Naskar and M. D. Dadmun, *ACS Appl. Mater. Interfaces*, 2016, **8**, 3200–3207.
- 20 D. R. Ratnaweera, D. Saha, S. V. Pingali, N. Labbe, A. K. Naskar and M. Dadmun, *RSC Adv.*, 2015, **5**, 67258–67266.
- 21 W. Zhao, L.-P. Xiao, G. Song, R.-C. Sun, L. He, S. Singh, B. A. Simmons and G. Cheng, *Green Chem.*, 2017, **19**, 3272–3281.
- 22 S. V. Pingali, H. M. O'Neill, Y. Nishiyama, L. L. He, Y. B. Melnichenko, V. Urban, L. Petridis, B. Davison and P. Langan, *Cellulose*, 2014, **21**, 873–878.
- 23 W. Zhao, B. Simmons, S. Singh, A. Ragauskas and G. Cheng, *Green Chem.*, 2016, **18**, 5693–5700.
- 24 A. P. Richter, J. S. Brown, B. Bharti, A. Wang, S. Gangwal, K. Houck, E. A. Cohen Hubal, V. N. Paunov, S. D. Stoyanov and O. D. Velev, *Nat. Nanotechnol.*, 2015, **10**, 817.
- 25 M. Lievonon, J. J. Valle-Delgado, M.-L. Mattinen, E.-L. Hult, K. Lintinen, M. A. Kostianen, A. Paananen, G. R. Szilvay, H. Setälä and M. Osterberg, *Green Chem.*, 2016, **18**, 1416–1422.
- 26 D. Tian, J. Hu, R. P. Chandra, J. N. Saddler and C. Lu, *ACS Sustainable Chem. Eng.*, 2017, **5**, 2702–2710.
- 27 O. U. Rahman, S. B. Shi, J. H. Ding, D. L. Wang, S. Ahmad and H. B. Yu, *New J. Chem.*, 2018, **42**, 3415–3425.
- 28 W. Yang, E. Fortunati, D. Gao, G. M. Balestra, G. Giovanale, X. He, L. Torre, J. M. Kenny and D. Puglia, *ACS Sustainable Chem. Eng.*, 2018, **6**, 3502–3514.
- 29 N. T. K. Thanh, N. Maclean and S. Mahiddine, *Chem. Rev.*, 2014, **114**, 7610–7630.
- 30 A. P. Richter, B. Bharti, H. B. Armstrong, J. S. Brown, D. Plemmons, V. N. Paunov, S. D. Stoyanov and O. D. Velev, *Langmuir*, 2016, **32**, 6468–6477.
- 31 K. Lintinen, Y. Xiao, R. Bangalore Ashok, T. Leskinen, E. Sakarinen, M. Sipponen, F. Muhammad, P. Oinas, M. Osterberg and M. Kostianen, *Green Chem.*, 2018, **20**, 843–850.
- 32 S. Salentinig and M. Schubert, *Biomacromolecules*, 2017, **18**, 2649–2653.
- 33 L. Mu, Y. Shi, H. Wang and J. Zhu, *ACS Sustainable Chem. Eng.*, 2016, **4**, 1840–1849.
- 34 K. Kratz, T. Hellweg and W. Eimer, *Polymer*, 2001, **42**, 6631–6639.
- 35 B. Hammouda, D. Ho and S. Kline, *Macromolecules*, 2002, **35**, 8578–8585.
- 36 S. Contreras, A. R. Gaspar, A. Guerra, L. A. Lucia and D. S. Argyropoulos, *Biomacromolecules*, 2008, **9**, 3362–3369.
- 37 O. Myrvold Bernt, *Holzforschung*, 2015, **69**, 9.
- 38 J. Sameni, S. Krigstin and M. Sain, *BioResources*, 2017, **12**, 1548–1565.
- 39 Y. Deng, X. Feng, M. Zhou, Y. Qian, H. Yu and X. Qiu, *Biomacromolecules*, 2011, **12**, 1116–1125.
- 40 J. Sun, T. Dutta, R. Parthasarathi, K. H. Kim, N. Tolic, R. K. Chu, N. G. Isern, J. R. Cort, B. A. Simmons and S. Singh, *Green Chem.*, 2016, **18**, 6012–6020.
- 41 F. Lu and J. Ralph, *J. Agric. Food Chem.*, 1998, **46**, 547–552.
- 42 A. K. Lewis, K. M. Dunleavy, T. L. Senkow, C. Her, B. T. Horn, M. A. Jersett, R. Mahling, M. R. McCarthy, G. T. Perell, C. C. Valley, C. B. Karim, J. Gao, W. C. K. Pomerantz, D. D. Thomas, A. Cembran, A. Hinderliter and J. N. Sachs, *Nat. Chem. Biol.*, 2016, **12**, 860–866.
- 43 T. M. Garver and P. T. Callaghan, *Macromolecules*, 1991, **24**, 420–430.
- 44 U. Vainio, N. Maximova, B. Hortling, J. Laine, P. Stenius, L. K. Simola, J. Gravitis and R. Serimaa, *Langmuir*, 2004, **20**, 9736–9744.
- 45 C. Maffi, M. Baiesi, L. Casetti, F. Piazza and P. De Los Rios, *Nat. Commun.*, 2012, **3**, 1065.
- 46 G. Cheng, Y. B. Melnichenko, G. D. Wignall, F. Hua, K. Hong and J. W. Mays, *Macromolecules*, 2008, **41**, 9831–9836.
- 47 C. Crestini, F. Melone, M. Sette and R. Saladino, *Biomacromolecules*, 2011, **12**, 3928–3935.
- 48 J. S. Pedersen, *Adv. Colloid Interface Sci.*, 1997, **70**, 171–210.
- 49 J. Zakzeski, P. C. A. Bruijninx, A. L. Jongerius and B. M. Weckhuysen, *Chem. Rev.*, 2010, **110**, 3552–3599.
- 50 J. P. Mata, P. A. Reynolds, E. P. Gilbert and J. W. White, *Colloids Surf., A*, 2013, **418**, 157–164.
- 51 J. Bahadur, C. R. Medina, L. He, Y. B. Melnichenko, J. A. Rupp, T. P. Blach and D. F. R. Mildner, *J. Appl. Crystallogr.*, 2016, **49**, 2021–2030.

